62/18

ARCHIWUM ODLEWNICTWA
Rok 2006, Rocznik 6, Nr 18 (1/2)
ARCHIVES OF FOUNDRY
Year 2006, Volume 6, N° 18 (1/2)
PAN – Katowice PL ISSN 1642-5308

EFFECT OF COOLING SPEED ON PRIMARY STRUCTURE OF B-1900 NICKEL-BASE SUPERALLOY

A. SZCZOTOK[1], J. SZALA[2], J. CWAJNA[3], M. HETMAŃCZYK[4]
Politechnika Śląska, Katedra Nauki o Materiałach, Katowice 40-019, ul. Krasińskiego 8

SUMMARY

The cast nickel-base superalloy B-1900 is used in gas turbine vane owing to its excellent high temperature strength and thermal fatigue resistance.
The article contains description of experimental method for evaluation of cooling speed effect on a microstructure of B-1900 superalloy, in particularly on secondary dendrite arm spacing as well as size and shape of primary carbides.

Key words: nickel-base superalloy, primary structure, cooling speed.

1. INTRODUCTION

Speed of carrying away of heat from solidifying casts have an essential influence on their primary structure. There has been a considerable interest in determining the effect of solidification variables on secondary dendrite arm spacing [1-7]. The interest is resulted from the fact that secondary dendrite arm spacing determines the micro-segregation pattern and that the cooling rate can be estimated from the secondary arm spacing of cast alloys. However, intensity of occurring changes depends on peculiarity of given material.

2. MATERIAL AND METHODOLOGY

In the presented work specimens made of heat-resisting B-1900 nickel-base alloy were analysed. B-1900 alloy is marked by high creep resistance as well as good oxidation

[1] *mgr inż., agnieszka.szczotok@polsl.pl*
[2] *dr hab. inż., janusz.szala@polsl.pl*
[3] *prof. dr hab. inż., jan.cwajna@polsl.pl*
[4] *prof. dr hab. inż., marek.hetmanczyk@polsl.pl*

resistance in high temperatures. On account of these properties it is applied to production of elements exploited in hot section of air engine exposed to „hot corrosion" [8-9]. During researches morphology of dendrites and carbide phase was analysed in function of the alloy's solidification speed.
Chemical composition of the B-1900 alloy is presented in Table 1.

Table 1. Chemical composition of B-1900 nickel-base alloy
Tabela 1. Skład chemiczny stopu na osnowie niklu B-1900

Elements contents [wt. %]									
B-1900	Ni	Cr	Co	Mo	Ta	Ti	Al	B	Zr
	bal.	8.00	10.00	6.00	4.25	1.00	6.00	0.015	0.07

Various solidification speeds of the analysed specimens were obtained using forming step cast (Fig. 1) of thickness: 6.8 mm (stairs a and b), 3.6 mm (c, d) and 2.3 mm (e, f) respectively. Selection of these steps thickness was dictated by dimensions of cross-sections the most frequently occurring in casts formed from B-1900. Metallographic sections from the samples b, d, e, marked by arrows in Fig. 1, were analysed.

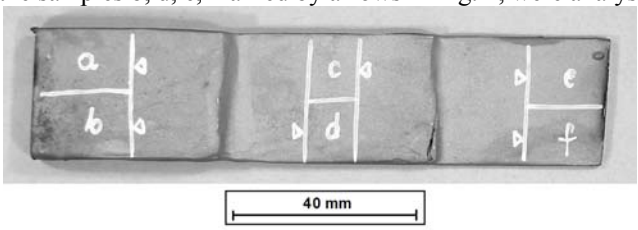

Fig. 1. Three-step sample with marked cutting lines
Rys. 1. Trójstopniowa próbka z zaznaczonymi liniami cięcia

Procedure of cutting, mounting, grinding and polishing of the specimens was carried out according to the recommendations of Buehler expert system [10] for nickel-base superalloys. A great difference of natural reflectiveness of carbides and metal matrix of this material enables to conduct a quantitative evaluation of carbide phase using computer methods on not etched specimens.
Images of a structure were registered using light microscope Olympus GX71 in dark field technique and using electron scanning microscope Hitachi S-4200. In both cases ten images from each specimen were registered. Images of the structure obtained using the light microscope were used for a quantitative description of eutectic areas occurring in the B-1900 alloy and for evaluation of secondary dendrite arm spacing. In the images obtained using the scanning microscope a quantitative evaluation of a carbide phase was made. All the measurements were executed using Met-Ilo programme [11].

Detection of the carbide phase on the images obtained from the light microscope consists in automatic binarization using maximum of histogram variance.
The binary images of the carbides obtained this way were used for detection of eutectic areas formed by these carbides. On the basis of the earlier researches it was assumed

that eutectic area is created by concentrations of carbides fulfilling one of two conditions:

- contains at least 5 carbides occurring in distance not greater than 5 pixels (in Fig. 2 procedure which can reveal these carbides was named: select_object_number (a,x=>5)),
- at least 2 holes occur in them (in Fig. 2: select_object_holes (a,=>2)).

Description of the most important elements of a procedure enabling to automate this process is presented in Fig. 2.

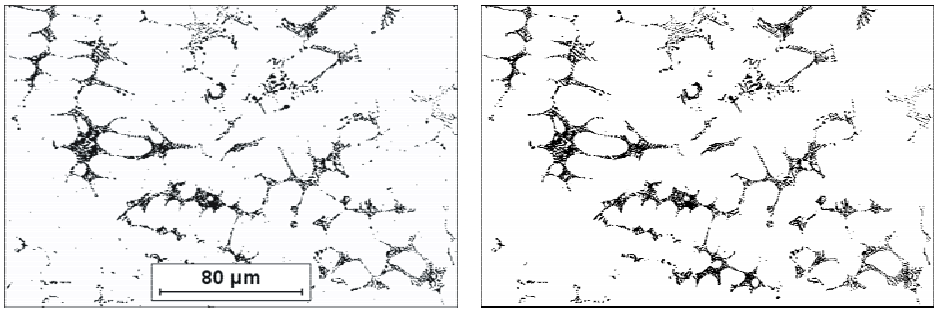

Image a – initial image

Image b
b = select_object_holes (a, =>2)

Image c
x = closing (a,5)
c = select_object_number (a,x =>5)

Image d – final image of eutectic areas (grey and black) and carbides (grey)
x = images_or (b,c)
d = closing (a,5)
d = reconstruction (d,x)

Fig. 2. Procedure of carbide eutectic areas detection on images of B-1900 alloy structure registered using light microscope

Rys. 2. Procedura detekcji obszarów eutektyk węglikowych na obrazach struktury stopu B-1900 z wykorzystaniem mikroskopu świetlnego

The eutectic areas were characterized using plane section areas and length of chords cut on them by a testing line. In both cases histograms of these parameters have been

worked out as well as their mean values designated as $\bar{a}$ and $\bar{l}$ respectively and coefficients of variation CV(a) and CV(l) have been evaluated. In addition area fraction (A_A) of eutectic areas has been calculated.

In the case of these structures it can be assumed that secondary dendrite arm spacing (λ_2) corresponds with minimum of Feret diameter of interdendritic areas. Almost all secondary dendrite arms visible on the structure images obtained using light microscope are not fully developed. Accordingly, their detection was carried out manually by a specialist experienced in range of heat-resisting nickel-base superalloys structure analysis. Distributions of secondary dendrite arm spacing as well as mean value of this parameter ($\bar{\lambda}_2$) and coefficient of variation CV(λ_2) have been obtained as a result of the measurement for each specimen.

There were not these problems during a detection of carbides on the images obtained with scanning microscope. This procedure was realized automatically using multiple binarization.

3. RESULTS

Results of the quantitative evaluation of the structure visible on the images registered using the light microscope (selected images are presented in Fig. 3) shown in Table 2 and in Fig. 4 indicate that speed of solidification affect morphology of dendrites and eutectic areas occurring in the B-1900 alloy specimen.

The greatest changes concern an interdendritic eutectic area. Growth of crystallization speed resulted in distinct decrease of these areas dimension described as a function of a mean area and a mean chord of their plane section area. However, homogeneity of these parameters does not change, which is testified by similar CV(a) and CV(l) values of all the samples. Small decrease of interdendritic eutectic area's fraction A_A with growth of solidification speed has also been observed. On the basis of only three specimens it is difficult to unequivocally claim that this tendency is permanent. It requires additional researches.

Along with decrease of the specimens thickness also secondary dendrite arm spacing reduces. Similarly as in case of interdendritic eutectic area, value of CV(λ_2) does not change. Character of λ_2 histogram does not also change; there is only displacement of maximum on this graph to lower values along with the decrease of specimen thickness.

Speed of the solidification affects also morphology of the eutectic carbides revealed on the images obtained using the scanning microscope.

This phenomenon is difficult to notice while comparing other images of specimens of various thickness (Fig. 3). Change of this phase's morphology is visible in the results of quantitative structure evaluation (Table 3).

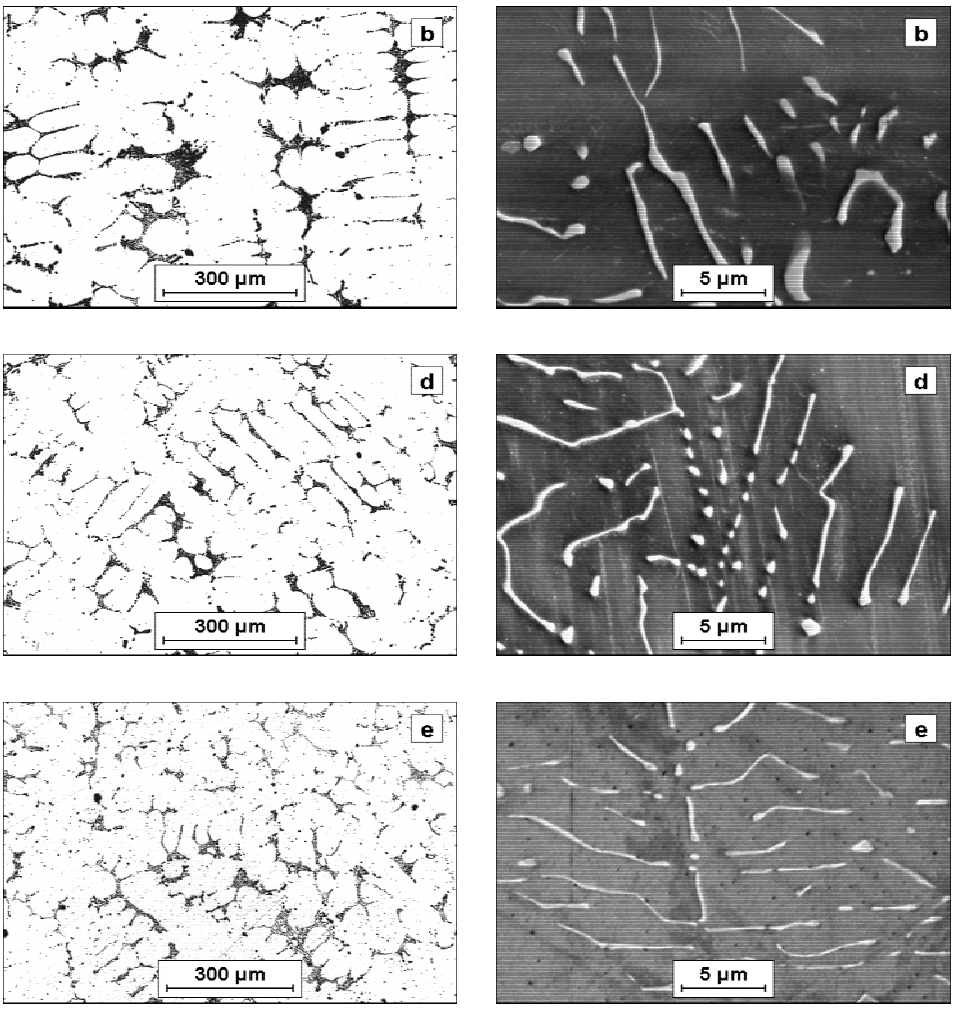

Fig. 3. Selected images of investigated specimens' structure. Light microscope – dark field technique (left) and scanning microscope (right). Letters mark a specimen symbol

Rys. 3. Wybrane obrazy struktury badanych próbek. Mikroskop świetlny – technika pola ciemnego (po lewej) i mikroskop skaningowy (po prawej). Litery oznaczają symbol próbki

With growth of the solidification speed dimension of carbides characterized as a mean area of their plane section areas $\overline{a}$ decreases. Quite marked changes of these

precipitations' dimensions inhomogeneity have been observed as well. Simultaneously there is no significant changes of the analysed precipitations' shape.

Table 2. Results of secondary dendrite arm spacing and interdendritic eutectic area quantitative evaluation

Tabela 2. Wyniki ilościowej oceny odległości między ramionami wtórnymi dendrytów i obszaru eutektyki międzydendrytycznej

Specimen	Secondary dendrite arm spacing (λ_2)		Interdendritic eutectic area				
	$\bar{\lambda}_2$ [µm]	CV(λ_2)	$\bar{a}$ [µm^2]	CV(a)	$\bar{l}$ [µm]	CV(l)	A_A [%]
b 6.8 mm	73.3	0.28	1520	2.17	20.0	1.03	10.2
d 3.6 mm	56.2	0.28	1108	2.31	15.7	1.05	9.9
e 2.3 mm	49.6	0.31	615	2.10	12.8	0.97	9.5

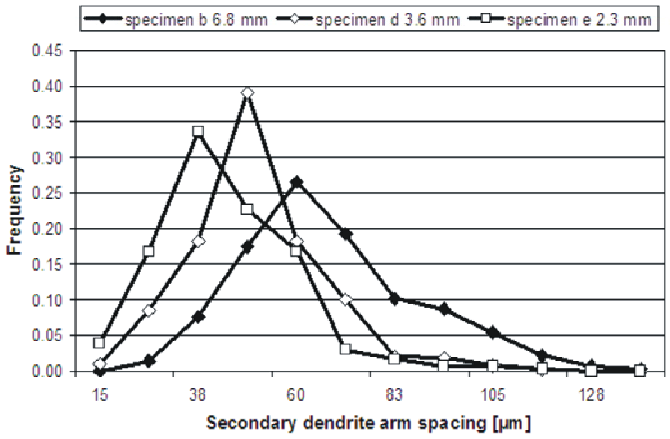

Fig. 4. Distributions of secondary dendrite arm spacing

Rys. 4. Rozkłady odległości między ramionami wtórnymi dendrytów

Table 3. Results of quantitative carbides evaluation occurring in eutectic areas

Tabela 3. Wyniki ilościowej oceny węglików występujących w obszarach eutektycznych

Specimen	$\bar{a}$ [µm^2]	CV(a)	$\bar{f}$	CV(f)
b 6.8 mm	2.21	1.41	0.54	0.58
d 3.6 mm	1.29	2.17	0.58	0.59
e 2.3 mm	0.58	1.10	0.58	0.59

4. CONCLUSIONS

The conducted researches confirmed essential influence of the B1900 alloy specimens solidification speed on their microstructure. Growth of the solidification speed results first of all in decrease of mean plane section area of eutectics. Changes of similar character occur also in case of secondary dendrite arm spacing and size of the carbides occurring in the eutectic areas. The methodology of eutectic areas detection proposed in the work enables automatic measurement process of this structural element.

ACKNOWLEDGEMENTS

Scientific work funded by the Scientific Research Committee in the years 2003-2005 as a research project No. 6 T08 2003C/06083.

REFERENCES

[1] T.Z. Kattamis, J.C. Coughlin, M.C. Flemings: *Influence of coarsening on dendrite arm spacing of aluminum-copper alloys.* Trans. Metal. 239, 1967.
[2] A.A. Chernov: *Estimation of the time of re-formation of inclusions in dendritic crystals.* Kristallografiya 1, 1956.
[3] J. Alkemper, R. Mendoza, P.W. Voorhees: *Morphological evolution of dendritic microstructures.* Advanced Engineering Materials 4, 2002.
[4] T. Suzuki, M. Ode, S.G. Kim, W.T. Kim: *Phase-field model of dendritic growth*. Journal of Crystal Growth 237-239, 2002.
[5] R.M. Sharp, A.J. Hellawell: *Solute distributions at non-planar solid-liquid growth fronts. IV. Ripening of cells and dendrites behind the growth front*. Journal of Crystal Growth 11, 1971.
[6] M. El-Bealy, B.G. Thomas: *Prediction of dendrite arm spacing for low alloy steel casting processes*. Metallurgical And Materials Transactions B 27, 1996.
[7] M. Chen, T.Z. Kattamis: *Dendrite coarsening during directional solidification of Al-Cu-Mn alloys.* Materials Science and Engineering A 247, 1998.
[8] A. Hernas: *Heat-resistance of steels and alloys* (in Polish). Gliwice, Poland: Silesian Technical University, 1999.
[9] M.J. Donachie, S.J. Donachie: *Superalloys - A Technical Guide*. Ohio, USA: ASM International, Materials Park, 2002.
[10] Buehler Ltd. *Buehler's Guide to Materials Preparation*. Illinois, USA: The Argus Press, Niles, 2002.
[11] J. Szala: *Application of computer-aided image analysis methods for a quantitative evaluation of material structure* (in Polish). Gliwice, Poland: Silesian Technical University, 2001.

WPŁYW SZYBKOŚCI KRZEPNIĘCIA NA STRUKTURĘ PIERWOTNĄ NADSTOPU B-1900 NA OSNOWIE NIKLU

STRESZCZENIE

Odlewniczy nadstop B-1900 na osnowie niklu jest wykorzystywany na łopatki kierujące turbin gazowych dzięki jego znakomitym własnościom wytrzymałościowym w wysokiej temperaturze i odporności na zmęczenie cieplne.
W artykule opisano eksperymentalną metodykę oceny wpływu szybkości krzepnięcia na mikrostrukturę nadstopu B-1900, w szczególności na odległość między ramionami wtórnymi dendrytów, jak również wielkość i kształt węglików pierwotnych.

Recenzował: Prof. Władysław Orłowicz